PHYSICAL REVIEW B **81**, 174535 (2010)

Interference patterns of multifacet 20×(0-π) Josephson junctions with ferromagnetic barrier

S. Scharinger,[1] C. Gürlich,[1] R. G. Mints,[2] M. Weides,[3,*] H. Kohlstedt,[4] E. Goldobin,[1] D. Koelle,[1] and R. Kleiner[1]
[1]*Physikalisches Institut–Experimentalphysik II and Center for Collective Quantum Phenomena, Universität Tübingen, Auf der Morgenstelle 14, D-72076 Tübingen, Germany*
[2]*The Raymond and Beverly Sackler School of Physics and Astronomy, Tel Aviv University, Tel Aviv 69978, Israel*
[3]*Institute of Solid State Research and JARA–Fundamentals of Future Information Technology, Research Center Jülich, D-52425 Jülich, Germany*
[4]*Nanoelektronik, Technische Fakultät, Christian-Albrechts-Universität zu Kiel, D-24143 Kiel, Germany*
(Received 12 March 2010; published 27 May 2010)

We have realized multifacet Josephson junctions with periodically alternating critical current density (MJJs) using superconductor-insulator-ferromagnet-superconductor heterostructures. We show that anomalous features of critical current vs applied magnetic field, observed also for other types of MJJs, are caused by a nonuniform flux density (parallel to the barrier) resulting from screening currents in the electrodes in the presence of a (parasitic) off-plane field component.

DOI: 10.1103/PhysRevB.81.174535 PACS number(s): 74.50.+r, 85.25.Cp, 74.78.Fk

I. INTRODUCTION

Multifacet Josephson junctions (MJJs), with critical current density j_c alternating many times between positive j_c^0 and negative $j_c^\pi \approx -j_c^0$ values along the junction were intensively treated during the last years. Initial studies were motivated by the discovery of high-T_c superconductors (cuprates) with d-wave order-parameter symmetry.[1] In thin-film cuprate grain-boundary junctions with a 45° misalignment angle between the two electrodes the current j_c is changing its sign randomly on a scale of a facet. A more controlled MJJ can be produced in the form of Nb/cuprate ramp junctions where the barrier forms a zigzag line parallel to the cuprate crystallographic axes.[2–4]

A more general interest in MJJs came from the possibility to have a *ground state* where the Josephson phase has a value φ different from both 0 and π,[5–9] or to realize tunable plasmonic crystals.[10] If a φ junction is long compared to the Josephson length λ_J it may carry *mobile* fractional flux quanta (splintered vortices).[11–14] A promising option to produce an MJJ is given by the superconductor-insulator-ferromagnet-superconductor (SIFS) technology,[15–17] providing exponentially low damping at low temperatures and a high topological flexibility in arranging the 0 and π segments. Recent imaging of the supercurrent distribution showed that in SIFS (Ref. 18) j_c is more homogeneous than in Nb/cuprate zigzag MJJs.[4]

The dependence of the critical current I_c on the applied field H for an MJJ is very different from usual Josephson junctions. If $j_c^\pi = -j_c^0$ and the facets have equal size, $I_c = 0$ in zero field but becomes large when the field causes constructive interference of the supercurrents flowing through the 0 and π segments. Standard calculations of $I_c(H)$ for a junction of length L and width W, assuming that the flux density B is homogeneous in the tunneling barrier and $L, W \lesssim 4\lambda_J$, show that the main peaks occur if the flux per facet is $\pm\Phi_0/2$ (Φ_0 is the flux quantum), resulting in the maximum current $I_c = 2LWj_c^0/\pi$. The other maxima in $I_c(H)$ are much lower and look symmetric relative to the main I_c maxima.[2]

Suppression of $I_c(0)$ and appearance of high-field main maxima were clearly observed for grain-boundary MJJs in a field perpendicular to the substrate plane.[19–21] Here, randomness in j_c^0, j_c^π and facet sizes prevent a close comparison to the "ideal" theoretical $I_c(H)$. However, differences between experiment and theory also appear for the more controllable zigzag MJJs. In particular, the secondary maxima between the two main maxima almost vanish in experiment and are strongly enhanced outside the main peaks.[2–4] These features cannot be reproduced in calculations by simply taking into account random nonuniformity of the junctions.

A major step toward understanding $I_c(H)$ was done in the framework of nonlocal electrodynamics of MJJs.[22] A universal solution has been found for $\phi(x)$ in the case when the electrodes are formed by an ultrathin film and the applied field is perpendicular to them (the definition of the coordinates is shown in Fig. 1). In this geometry, the flux density $B_z(x)$ is strongly enhanced compared to $\mu_0 H_z$, has a maximum in the center of the junction and decays to zero toward the edges, see Fig. 2(a) in Ref. 22 [the quantity $\phi_0'(Y)$ plotted there is proportional to the flux density along the junction, i.e., $B_z(x)$ in our notation]. As a result the main maxima of I_c are suppressed compared to the case of uniform B_z while the maxima following the main maximum are strongly enhanced, see Fig. 4(b) of Ref. 22.

In this paper we report the results of our study of $I_c(H)$ dependence of rectangular Nb|Al_2O_3|$Ni_{0.6}Cu_{0.4}$|Nb SIFS MJJ structures with length $L = 200$ μm and width $W = 10$ μm. Sections, consisting of 5 μm long 0-π segments are repeated $N = 20$ times, as sketched in Fig. 1. The total length $L \approx 3\lambda_J$, i.e., these MJJs can be treated as short junctions.

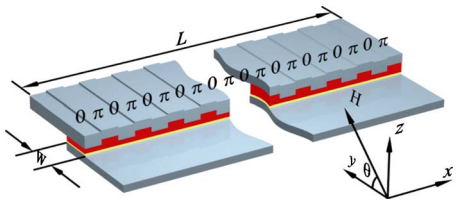

FIG. 1. (Color online) Sketch of a SIFS MJJ with 20 facets.

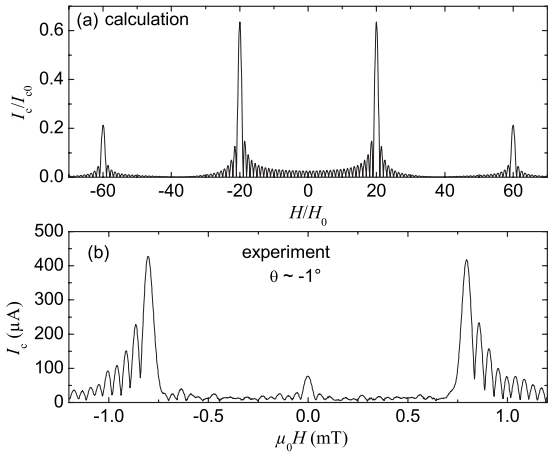

FIG. 2. (a) Calculated critical current of a 20×0-π MJJ as a function of applied field, for $j_c^0=|j_c^\pi|$, facets of equal size and a homogeneous field $\mathbf{B}\|\hat{y}$. (b) A "typical" experimental pattern (T=4.2 K), when $\boldsymbol{H}$ is misaligned relative to the substrate plane ($\theta\approx-1°$).

II. THEORY

In a short MJJ, see Fig. 1, the flux generated by tunneling currents is negligible. If B_y and j_c do not depend on y, I_c is given by

$$I_c = W \max_{\phi_0} \int_{-L/2}^{L/2} \{j_c(x)\sin[\phi(x,B_y)+\phi_0]\}dx. \qquad (1)$$

In what follows we consider complex interference patterns depending on the spatial distribution of flux inside the junction. Thus, to show the results of our numerical studies, we plot I_c/I_{c0} as a function of H/H_0, where $I_{c0}=j_c^0LW$ and $H_0=\Phi_0/\mu_0\Lambda L$. Λ is the (average) effective magnetic junction thickness accounting for flux penetration into the superconducting electrodes and the effect of screening currents. ($\Lambda\approx2\lambda_L$ for a junction in a bulk sample, where λ_L is the London penetration depth); below we will also allow Λ to be different in the 0 and π parts.

The phase $\phi(x,B_y)$ is obtained from the equation

$$\frac{d\phi}{dx} = \frac{2\pi B_y(x)\Lambda}{\Phi_0}, \qquad (2)$$

The calculated $I_c(H)$ for constant Λ and constant $B_y(x)=\mu_0 H$ is shown in Fig. 2(a). The two main maxima of I_c occur at $|H|/H_0=N$. The next maxima are located at $|H|/H_0=3N$. Further, $I_c=0$ at $|H|/H_0=2N$.

III. EXPERIMENT

The current-voltage curves of the MJJs that we studied experimentally at $T\approx4.2$ K are nonhysteretic. We determined I_c by using a voltage criterion $V_{cr}=1$ μV except for the data shown in Fig. 2(b), where we have used a different measurement setup, with $V_{cr}=0.2$ μV. Thus, we have an I_c detection limit (parasitic I_c background) $I_{cr}=V_{cr}/R$ ($R\approx0.05$ Ω). $I_{cr}\approx4$ μA in Fig. 2(b) and ≈20 μA in all other experiments. When the sample was aligned "by eye" to have

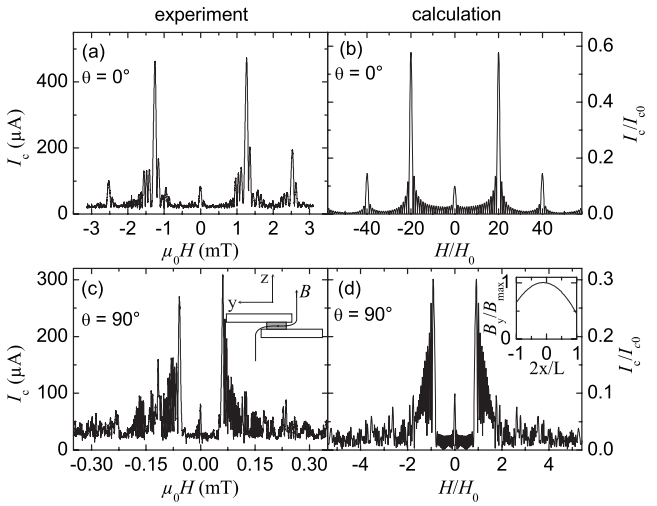

FIG. 3. $I_c(H)$ curves for [(a) and (b)] parallel ($\theta=0°$) and [(c) and (d)] perpendicular ($\theta=90°$) field orientation. Inset in (c) is a sketch of $\boldsymbol{B}$ in the (y,z) plane for $\theta=90°$. Inset in (d) shows the profile $B_y(x)$ used to calculate $I_c(H)$ for $\theta=90°$.

$\boldsymbol{H}\|\hat{y}$, the $I_c(H)$ patterns [see, e.g., Fig. 2(b); in comparison to Fig. 2(a) the applied field scale roughly corresponds to $\pm30H_0$] resembled the ones of zigzag junctions[2,3] (where $\boldsymbol{H}\|\hat{z}$), but not the calculated "ideal case" pattern shown in Fig. 2(a). In particular, the measured $I_c(H)$ shows a small local maximum at $H=0$ and high maxima following the main maxima.

The model considered in Ref. 22 (ultrathin film grain-boundary MJJ in the (x,y) plane) cannot be applied since (a) the geometry of SIFS MJJ is more complicated and (b) the validity conditions for the nonlocal model are not satisfied. However, for the SIFS (and also zigzag) MJJs an applied field $\boldsymbol{H}\|\hat{z}$ should be subject to field focusing effects, with a maximum of $B_y(x)$ in the center of the junction.[23,24] In our MJJ aligned "by eye" a component H_z may arise from a slight out-of-plane misalignment of the applied field. This small field leads to strong modifications of $I_c(H)$. To test this idea we measured $I_c(H)$ for different angles θ between $\boldsymbol{H}$ and the substrate plane (see Fig. 1), using two perpendicular coils operated in linear combination and creating $H_y=H\cos\theta$ and $H_z=H\sin\theta$.

Figure 3(a) shows $I_c(H)$ measured at an angle, which, after having measured and analyzed the angle dependent $I_c(H)$ (see below), has been identified to be very near $\theta=0°$. The shape of this curve is much closer to the "ideal case," although differences occur. First, there is an I_c maximum at $H=0$. This naturally arises, because, typically, $|j_c^\pi|\neq j_c^0$ and thus the cancellation of the supercurrents carried by the 0 and π parts is incomplete. Second, an I_c peak appears at $H/H_0=40=2N$. If both the 0 and π segments had the same length and the same Λ, at this field I_c should cancel within each segment. However, e.g., due to the different fabrication of the Nb top layer, the Nb mean-free path and thus also Λ may slightly differ for the 0 and π parts.[25] Then, I_c cannot cancel at the same field in both the 0 and the π segments and a peak may appear in $I_c(H)$. Further note that the measured $I_c(H)$ is asymmetric with respect to positive and negative H. This

effect arises from asymmetries in the ferromagnet layer magnetization which we do not take into account to keep the discussion short.

Taking asymmetries of j_c and different values Λ_0 and Λ_π of the 0 and π parts into account, using Eqs. (1) and (2), we calculate the $I_c(H)$ pattern shown in Fig. 3(b). In Fig. 3(b) we have used $\Lambda_\pi/\Lambda_0=1.38$ and $j_c^\pi/j_c^0=-0.8$ to achieve the best fit to the experimental curve. This translates to $j_c^0 \approx 42$ A/cm^2 and $j_c^\pi \approx -34$ A/cm^2 in physical units. These parameters are reasonable and the resulting $I_c(H)$ describes the data well. Also note that the ratios j_c^π/j_c^0 and Λ_π/Λ_0 can be determined independently and in a straightforward way, by analyzing the I_c maxima at, respectively, $H=0$ and $H=20H_0$. Comparing the field axes of Figs. 3(a) and 3(b) we obtain $\Lambda_0 \approx 134$ nm and $\Lambda_\pi \approx 186$ nm in reasonable agreement with the value of $2\lambda_L$ ($\lambda_L \approx 90$ nm for Nb). Further, using

$$\lambda_J^i = \sqrt{\Phi_0/2\pi\mu_0|j_c^i|d'}, \quad \text{with} \quad i=0,\pi, \tag{3}$$

we find a normalized junction length $l \equiv L/2\lambda_J^0 + L/2\lambda_J^\pi \approx 3.2$, i.e., this MJJ is in the short limit. In Eq. (3), $\mu_0 d'$ is the inductance per square (with respect to in-plane currents) of the electrodes and $d' \approx \Lambda$ for electrode thicknesses $\gtrsim \lambda_L$.

Having analyzed $I_c(H_y)$ and fixed the junction parameters j_c^0, j_c^π, Λ_0, and Λ_π we turn to the other limit of $\boldsymbol{H}\|\hat{z}$, ($\theta=90°$). The corresponding measured $I_c(H)$ pattern is shown in Fig. 3(c). Its shape resembles the ones of zigzag junctions[2–4] or of the SIFS MJJ with $\boldsymbol{H}\|\hat{y}$ aligned "by eye," cf. Fig. 2(b). Note that our MJJ is sensitive to H_z, because screening currents flowing inside the electrodes create a nonuniform field component $B_y(x)$ inside the junction barrier, as sketched in the inset of Fig. 3(c). To calculate $I_c(H_z)$ we need to find a profile $B_y(x)$ caused by the applied field $\boldsymbol{H}\|\hat{z}$ and solve Eqs. (1) and (2) using this $B_y(x)$. Similar to the case of a 0 junction having overlap geometry[23,24] and to the nonlocal grain-boundary junction[22] we expect $B_y(x)$ to have a maximum in the center of the MJJ ($x=0$). It can be approximated as[22–24] $B_y(x) \propto \cos(\pi x/L)$ if the junction is "naked," i.e., without idle regions surrounding the Josephson barrier. In our case there are 5 μm wide idle regions. Then, B_y will be nonzero at $x=\pm L/2$. In addition, asymmetries in $B_y(x)$ may occur due to asymmetries in the junction layout. Thus, we approximate $B_y(x)$ by a Taylor expansion near $x=0$, i.e., $B_y(x)=-f\mu_0 H_z(1+a_1\xi+a_2\xi^2)$, where $\xi=2x/L$ and $-1<\xi<1$. Solving Eq. (1), we get the $I_c(H)$ pattern shown in Fig. 3(d). We have used $a_1=-0.1$ and $a_2=-0.45$ to reproduce the data. While the overall shape of $I_c(H)$ strongly depends on the value of a_2, the nonzero choice of a_1 is somewhat cosmetic and was merely necessary to suppress a "shoulder" in the calculated $I_c(H)$ oscillations appearing for flux values above the main I_c maximum. For lower values of H this parameter has only a small effect on I_c. The resulting field profile is shown in the inset of Fig. 3(d). Further, by comparing the abscissas of the calculated and experimental curves, we find a field focusing factor $f \approx 23$, which is a reasonable value for the large MJJ we study.

Having reproduced $I_c(H)$ for both $\boldsymbol{H}\|\hat{y}$ and $\boldsymbol{H}\|\hat{z}$, we consider the general case where $\boldsymbol{H}$ is tilted by an angle θ. No additional parameters are required for calculating $I_c(H)$. We obtain

$$B_y(\xi) = -\mu_0 H[(f\sin\theta - \cos\theta) + (a_1\xi + a_2\xi^2) f\sin\theta]. \tag{4}$$

Similar to the geometries analyzed in Refs. 24 and 26 at a "dead angle" $\theta_d=\arctan(1/f)$ the uniform field term vanishes and one obtains an anomalous $I_c(H)$ dependence with diverging period. The linear and quadratic terms in $B_y(x)$ can have different signs relative to the constant term depending on θ. For angles between θ_d and 0°, and for a negative coefficient a_2, $B_y(x)$ peaks at the junction edges while at all other angles the maximum in B_y is in the junction center.

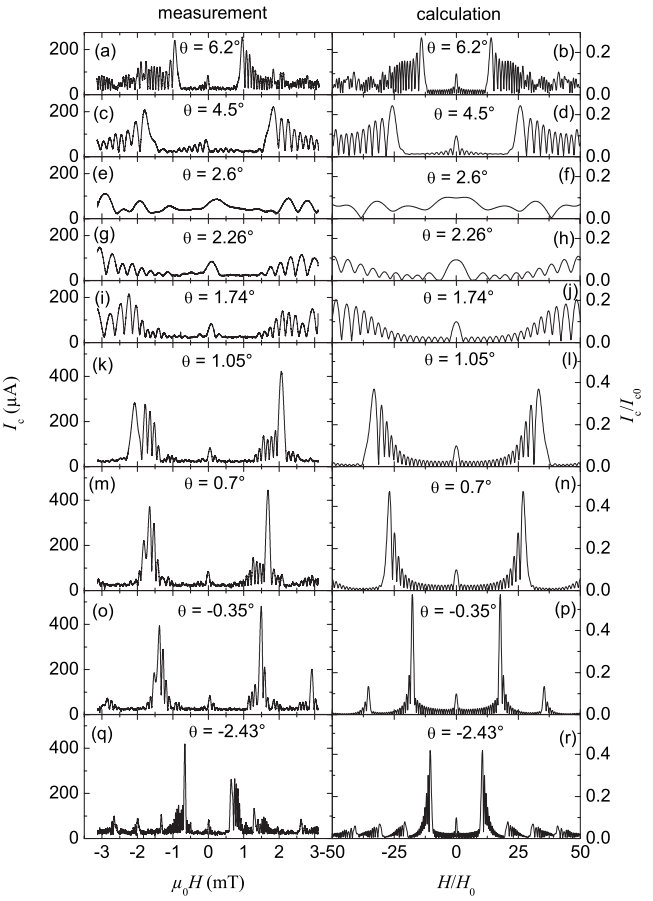

FIG. 4. $I_c(H)$ patterns for different misalignment angles θ.

In Fig. 4 we show a sequence of $I_c(H)$ patterns starting from $\theta=6.2$ to $\theta=-2.43°$ comparing the measured $I_c(H)$ with calculated curves. All data have been taken in a single cool down. In the simulated curves the junction parameters and coefficients a_1, a_2 are the same as for the cases $\theta=0°$ and $\theta=90°$ discussed above. The patterns taken at $\theta=6.2°$, see Fig. 4(a) differ only marginally from the case of $\theta=90°$, shown in Fig. 3(a). The main difference is the field scale due to the $\sin\theta$-reduced $B_y(x)$ field caused by H_z. In particular, for the cases $\theta=6.2°$ and $\theta=4.5°$ the enhancement of the higher order I_c maxima (relative to the main maximum) can nicely be seen. When approaching θ_d ($\approx 2.5°$ for our sample), $I_c(H)$ stretches anomalously with an increased amplitude of the

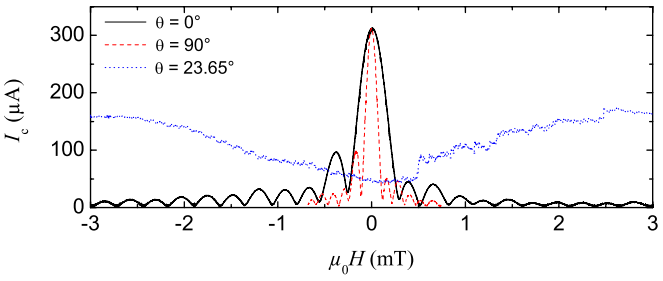

FIG. 5. (Color online) $I_c(H)$ curves for a 50×10 μm^2 SIFS 0 junction for $\theta=0°$, 90° and 23.65° ($\approx\theta_d$).

low-field I_c oscillation and with an increased field modulation period. Further, for angles between θ_d and 0° [where, according to Eq. (4), the field profile $B_y(x)$ reverses shape] the *lower* order I_c maxima become enhanced while the *higher* order maxima are suppressed. These features are well reproduced by the calculated curves $I_c(H)$. $I_c(H)$ at $\theta=0°$ is shown in Fig. 3(a). For negative values of θ the shape of $I_c(H)$ rapidly develops into the pattern found for $\boldsymbol{H}\|\hat{z}$, without anomalies at $\theta=-\theta_d$.

A "dead angle" has been found for 0 junctions of various geometries.[24,26] To further test this for SIFS junctions having large idle regions we have measured $I_c(H)$ of a 50 μm $\times10$ μm 0 coupled SIFS junction, for $\boldsymbol{H}$ applied under different angles θ. Figure 5 shows the resulting curves for three values of θ. For $\theta=0°$ and 90° $I_c(H)$ is close to a Fraunhofer pattern, with a compressed field scale for the $\theta=90°$ case; by comparing the modulation periods of these two curves we find $f\approx2.3$ and calculate $\theta_d\approx23.5°$. The dependence $I_c(H)$, measured at $\theta=23.65°$ and shown in Fig. 5, indeed is by no means Fraunhofer like.

The value of θ_d depends on the lead geometry via the field focusing factor f which is large for long junctions with wide leads. While $\theta_d\approx23.65°$, found for our 0 junction, is not very critical if the sample is aligned "by eye," other geometries, particularly in the context of long junction physics may have larger values of f and correspondingly lower values of θ_d.

IV. SUMMARY

We have studied a $20\times(0\text{-}\pi)$ multifacet SIFS Josephson junction. Its $I_c(H)$ dependence, when the applied magnetic field is aligned accurately parallel to the junction plane, can be described well by the standard linear phase ansatz (constant field), taking into account $|j_c^0|\neq|j_c^\pi|$ and different values for the effective magnetic junction thickness Λ in the 0 and π parts. On the other hand, a variety of $I_c(H)$ patterns can be obtained as a result of a small misalignment and field focusing. When the perpendicular field component dominates, the $I_c(H)$ patterns are similar to the ones measured for Nb/cuprate zigzag $0\text{-}\pi$ junctions. Specific features are: (a) a suppressed amplitude of the main I_c maxima and (b) a strong asymmetry between the lower order and higher order maxima. If the field is off-plane one may meet a "dead angle" θ_d where the flux density B_y caused by H_y is cancelled by the constant part of a nonuniform $B_y(x)$ induced by H_z. The effect is not restricted to multifacet SIFS junctions. If the sample is aligned so that $\theta\approx\theta_d$, $I_c(H)$ is anomalous and may lead to erroneous conclusions about the sample quality or even the physics investigated.

Although the MJJ investigated here has a too large j_c asymmetry to form a φ junction, the effects discussed here should be taken into account for the right interpretation of experimental results obtained for such devices in applied magnetic field.

ACKNOWLEDGMENTS

We acknowledge financial support of the German Israeli Foundation (Grant No. G-967-126.14/2007) and of the Deutsche Forschungsgemeinschaft (SFB/TRR 21 and Project No. WE 4359/1-1).

*Present address: Department of Physics, University of California, Santa Barbara, CA 93106, USA.

[1] C. C. Tsuei and J. R. Kirtley, Rev. Mod. Phys. **72**, 969 (2000).
[2] H.-J. H. Smilde, Ariando, D. H. A. Blank, G. J. Gerritsma, H. Hilgenkamp, and H. Rogalla, Phys. Rev. Lett. **88**, 057004 (2002).
[3] Ariando, D. Darminto, H. J. H. Smilde, V. Leca, D. H. A. Blank, H. Rogalla, and H. Hilgenkamp, Phys. Rev. Lett. **94**, 167001 (2005).
[4] C. Gürlich, E. Goldobin, R. Straub, D. Doenitz, Ariando, H.-J. H. Smilde, H. Hilgenkamp, R. Kleiner, and D. Koelle, Phys. Rev. Lett. **103**, 067011 (2009).
[5] A. Buzdin and A. E. Koshelev, Phys. Rev. B **67**, 220504(R) (2003).
[6] E. Goldobin, D. Koelle, R. Kleiner, and A. Buzdin, Phys. Rev. B **76**, 224523 (2007).
[7] A. Buzdin, Phys. Rev. Lett. **101**, 107005 (2008).
[8] A. Zazunov, R. Egger, T. Jonckheere, and T. Martin, Phys. Rev. Lett. **103**, 147004 (2009).
[9] A. Gumann and N. Schopohl, Phys. Rev. B **79**, 144505 (2009).
[10] H. Susanto, E. Goldobin, D. Koelle, R. Kleiner, and S. A. van Gils, Phys. Rev. B **71**, 174510 (2005).
[11] R. G. Mints, Phys. Rev. B **57**, R3221 (1998).
[12] R. G. Mints and I. Papiashvili, Phys. Rev. B **64**, 134501 (2001).
[13] R. G. Mints, I. Papiashvili, J. R. Kirtley, H. Hilgenkamp, G. Hammerl, and J. Mannhart, Phys. Rev. Lett. **89**, 067004 (2002).
[14] M. Moshe and R. G. Mints, Phys. Rev. B **76**, 140507(R) (2007).
[15] T. Kontos, M. Aprili, J. Lesueur, F. Genêt, B. Stephanidis, and R. Boursier, Phys. Rev. Lett. **89**, 137007 (2002).
[16] M. Weides, M. Kemmler, H. Kohlstedt, R. Waser, D. Koelle, R. Kleiner, and E. Goldobin, Phys. Rev. Lett. **97**, 247001 (2006).
[17] M. Weides, C. Schindler, and H. Kohlstedt, J. Appl. Phys. **101**, 063902 (2007).
[18] C. Gürlich, S. Scharinger, M. Weides, H. Kohlstedt, R. G. Mints,

E. Goldobin, D. Koelle, and R. Kleiner, Phys. Rev. B **81**, 094502 (2010).
[19] C. A. Copetti, F. Rüders, B. Oelze, C. Buchal, B. Kabius, and J. W. Seo, Physica C **253**, 63 (1995).
[20] J. Mannhart, H. Hilgenkamp, B. Mayer, C. Gerber, J. R. Kirtley, K. A. Moler, and M. Sigrist, Phys. Rev. Lett. **77**, 2782 (1996).
[21] H. Hilgenkamp and J. Mannhart, Rev. Mod. Phys. **74**, 485 (2002).
[22] M. Moshe, V. G. Kogan, and R. G. Mints, Phys. Rev. B **79**, 024505 (2009).
[23] R. Monaco, M. Aaroe, J. Mygind, and V. P. Koshelets, J. Appl. Phys. **104**, 023906 (2008).
[24] R. Monaco, M. Aaroe, J. Mygind, and V. P. Koshelets, Phys. Rev. B **79**, 144521 (2009).
[25] M. Kemmler, M. Weides, M. Weiler, M. Opel, S. T. B. Goennenwein, A. S. Vasenko, A. A. Golubov, H. Kohlstedt, D. Koelle, R. Kleiner, and E. Goldobin, Phys. Rev. B **81**, 054522 (2010).
[26] J. K. Heinsohn, R. Dittman, J. R. Contreras, E. Goldobin, A. M. Klushin, and M. Siegel, J. Appl. Phys. **90**, 4623 (2001).